Electronic Supplementary Material (ESI) for Physical Chemistry Chemical Physics.

Supporting Information

In Situ Examination of Charged Amino Acid-Induced Structural Change of Lipid Bilayers by Sum Frequency Generation Vibrational Spectroscopy

Jiahui Zhang,[a,b] Weilai Yang,[a] Junjun Tan[a,b] and Shuji Ye*[,a,b]

[a] Hefei National Laboratory for Physical Sciences at the Microscale, and Department of Chemical Physics, University of Science and Technology of China, Hefei, Anhui 230026, China,

[b] Synergetic Innovation Center of Quantum Information & Quantum Physics, University of Science and Technology of China, Hefei, Anhui 230026, China

1. Molecular structures of the lipids and amino acids under study

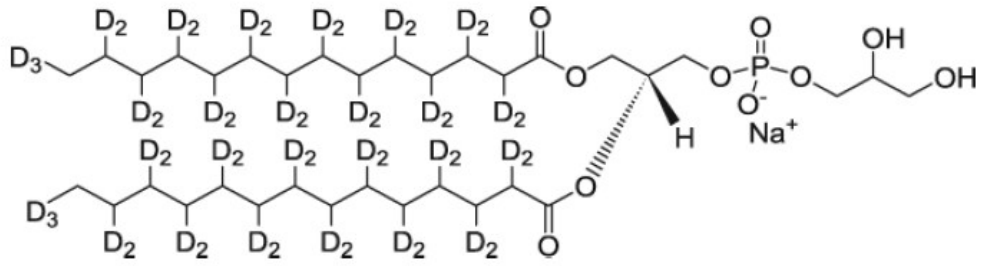

d-DMPG

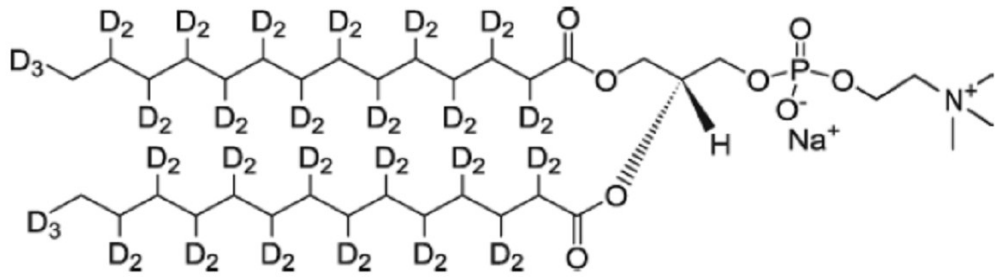

d-DMPC

Figure S1. Molecular structures of d-DMPG and d-DMPC.

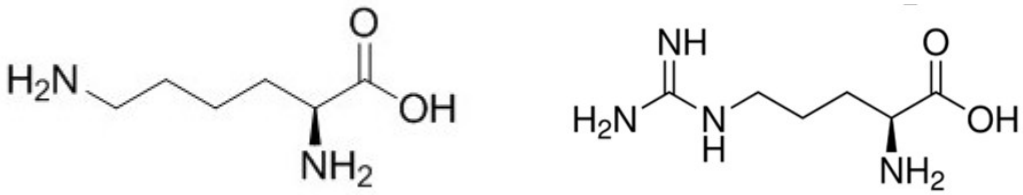

lysine arginine

Figure S2. Molecular structures of lysine and arginine.

2. The procedures of prism-cleaning and lipid monolayer/bilayer preparations

CaF_2 prisms were thoroughly cleaned using a procedure with several steps: They were first soaked in toluene for at least 24 h and then sonicated in soap detergent solution for 0.5 h. After that, they were rinsed with deionized (DI) water before soaking in methanol for 10 min. All of the prisms were then rinsed thoroughly with an ample amount of DI water and cleaned inside a Harrick plasma chamber for 10 min immediately before depositing lipid molecules on them. Substrates were tested using SFG, and no signal from contamination was detected.

Single lipid bilayers were prepared on CaF_2 substrates using Langmuir–Blodgett and Langmuir–Schaefer (LB/LS) methods with a KSV mini trough LB system. The processes are similar to the methods given by Chen Group.[1] Briefly, a sample holder was used to fasten the prism. One right-angle face of the prism was attached to a sample holder while the other right-angle face was perpendicularly immersed in the ultrapure water (prepared by a Millipore system: Millipore, Bedford, MA) inside the mini Langmuir trough.

To prepare the proximal leaflet (Figure 1), a certain amount of lipid solution was first carefully spread onto the water surface. After 5-10 minutes to allow the solvent of lipid to evaporate, the monolayer area was slowly compressed to a surface pressure of 35 mN/m by two barriers at a rate of 5 mm/min. The prism was then lifted out of the subphase at a rate of 2 mm/min. The prisms deposited with lipid monolayer were put in a clean small box before next-step experiments.

The distal leaflet was prepared in situ before doing SFG experiments. A 2.0-mL reservoir (prepared by Teflon) was placed in a large Teflon disc. The latter is slightly

deeper than the former. A monolayer of lipid at 35 mN/m surface pressure was formed by spreading a lipid solution onto a water surface. At this case, the prism's monolayer-coated right-angle face was horizontal to the water surface. The bilayer is formed by lowering the prism and allowing the prism's monolayer-coated right-angle face to contact the monolayer on the water surface. The extra lipids at the air/water interface were sucked away. The bilayer was immersed in water throughout the entire experiment, and a small amount of water could be added to the reservoir to compensate for evaporation when needed for long timescale experiments.

3. Fitting of the SFG-VS signals

The intensity of the SFG radiation is proportional to the square of the material's second-order susceptibility ($\chi_{eff}^{(2)}$), the intensity of the input visible beam ($I_1(\omega_{vis})$) and the intensity of the input IR beam ($I_2(\omega_{IR})$), as shown in Eq. (S1),[2-7]

$$I(\omega_{SFG}) \propto \left|\chi_{eff}^{(2)}\right|^2 I_1(\omega_{Vis}) I_2(\omega_{IR}) \tag{S1}$$

where $\omega_{SFG} = \omega_{IR} + \omega_{vis}$. For materials having inversion symmetry, the value of $\chi_{eff}^{(2)}$ is zero. No SFG signal would be generated in the bulk, whereas signals appear at the surface and interface due to the breakage of inversion symmetry. $\chi_{eff}^{(2)}$ is composed of two components: the effective surface nonlinear susceptibility ($\chi_R^{(2)}$) and the non-resonant background ($\chi_{NR}^{(2)}$). By properly tuning the frequency of the IR beam over the vibrational resonance of the surface/interface molecules, the value of $\chi_R^{(2)}$ can reach its maximum. $\chi_{eff}^{(2)}$ is frequency-dependent, as described in Eq. (S2),

$$\chi_{eff}^{(2)}(\omega) = \chi_{NR}^{(2)} + \sum_{\upsilon} \frac{A_\nu}{\omega - \omega_\nu + i\Gamma_\nu} \tag{S2}$$

where A_ν, ω_ν and Γ_ν refer to the strength, resonant frequency, and damping coefficient of the vibrational mode (ν), respectively. A_ν could be either positive or negative depending on the phase of the vibrational mode, and A_ν, ω_ν, and Γ_ν can be

extracted by fitting the spectrum.

4. Data analysis

Equations (S3)-(S6) present the relationship between the intensity ratio of $\chi^{(2)}_{ssp}(CD_3,as)/\chi^{(2)}_{ssp}(CD_3,ss)$ and the orientation angle of the CD_3 group (θ_{CD_3}), and the calculated curve is plotted in Figure S3.

$$\chi^{(2)}_{eff,ssp} = L_{yy}(\omega_{SFG})L_{yy}(\omega_{vis})L_{zz}(\omega_{IR})\sin\theta_{IR}\chi^{(2)}_{yyz} = C^{ssp}_{Fresnel}\chi^{(2)}_{yyz} \quad \text{(S3)}$$

$$\chi^{(2)}_{yyz}(CD_3,ss) = \frac{1}{2}N[(1+r)<\cos\theta> -(1-r)<\cos^3\theta>]\beta_{ccc} \quad \text{(S4)}$$

$$\chi^{(2)}_{yyz}(CD_3,as) = -N[<\cos\theta> - <\cos^3\theta>]\beta_{caa} \quad \text{(S5)}$$

$$r = \beta_{aac}/\beta_{ccc} \quad \text{(S6)}$$

where L_{ii} is the diagonal element of the Fresnel factor, θ_{IR} is the IR incident angle, and ω_{SFG}, ω_{vis}, and ω_{IR} refer to the frequencies of SFG, visible light and IR light, respectively.[2-7] $\beta_{lmn}(l,m,n=a,b,c)$ is the molecular hyperpolarizability. The average orientation angle (θ) can be determined by relating the SFG susceptibility tensor elements $\chi^{(2)}_{yyz}$ of the symmetric and asymmetric modes of CD_3. In terms of the reference 8, a relation between the $\chi^{(2)}_{ssp}(CD_3,as)/\chi^{(2)}_{ssp}(CD_3,ss)$ and θ_{CD_3} can be deduced using the value of r=2.3 and β_{caa}/β_{aac}=4.2 (Figure S3). Therefore, θ_{CD_3} can be easily obtained by knowing the ratio of $\chi^{(2)}_{ssp}(CD_3,as)/\chi^{(2)}_{ssp}(CD_3,ss)$.

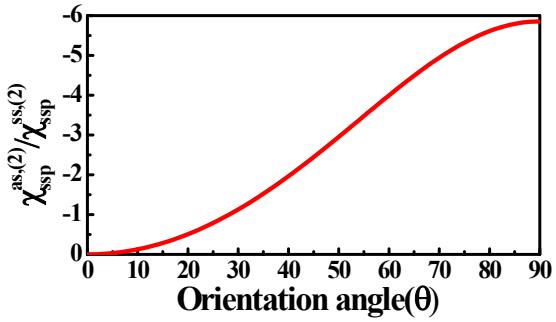

Figure S3. Relationship between $\chi^{(2)}_{ssp}(CD_3,as)/\chi^{(2)}_{ssp}(CD_3,ss)$ and θ_{CD_3}.

5. The evidence of water signals in the right tail of the spectra before and after adding amino acids into d-DMPG bilayer

The right tail in Figures 2A and 3A extends to very high frequency and connects to the water signals. Here, we assigned the right tails in the spectra to the contributions from water signals.

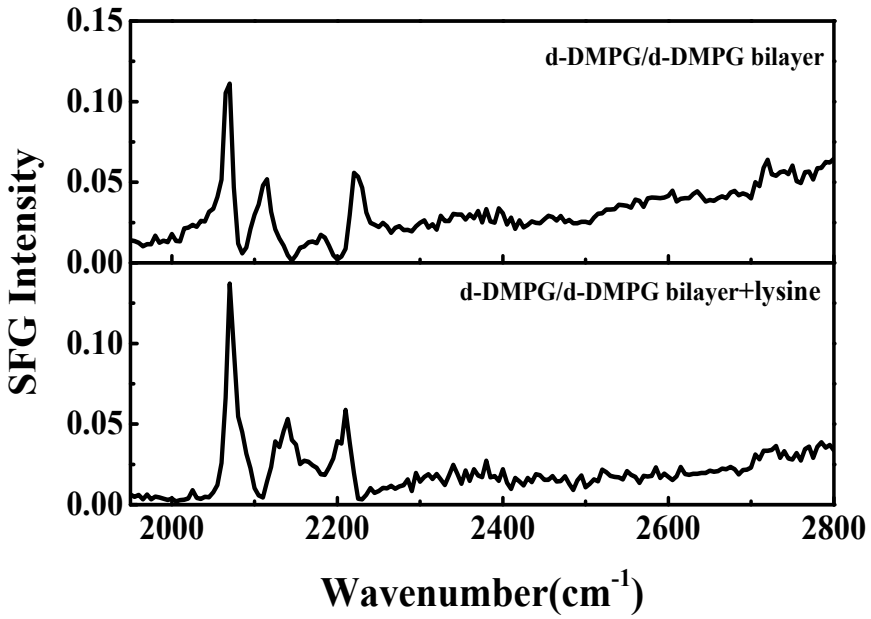

Figure S4. The ssp SFG spectra of d-DMPG bilayer in the frequency region of 1950-2800 cm^{-1} before (top) and after (bottom) injecting lysine.

6. The initial ssp SFG spectra in the PO_2^- ss region of the d-DMPG bilayer for the experiments of the injection of lysine and arginine before and after standardization using standard sample intensity.

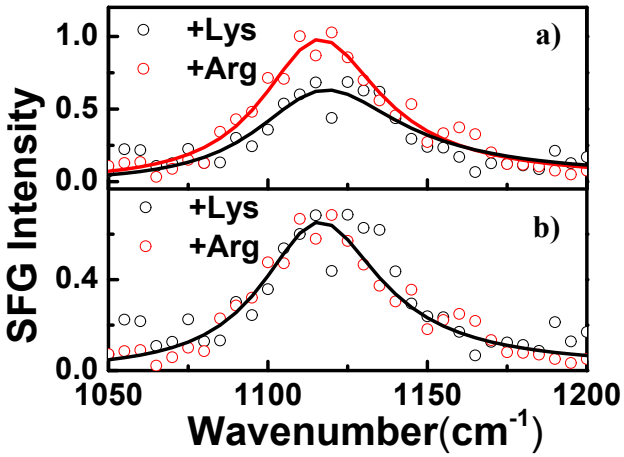

Figure S5. The initial ssp SFG spectra in the PO_2^-ss region of the d-DMPG bilayer for the experiments of the injection of lysine and arginine. a) before standardization using standard sample intensity; b) after standardization using standard sample intensity.

7. Signals of the carbonyl group from the amino acids

In Figure S6, the carbonyl group from the amino acid shows the signal in the range of 1550-1650 cm^{-1} and no absorption peak appears in the range of 1700-1800 cm^{-1}.

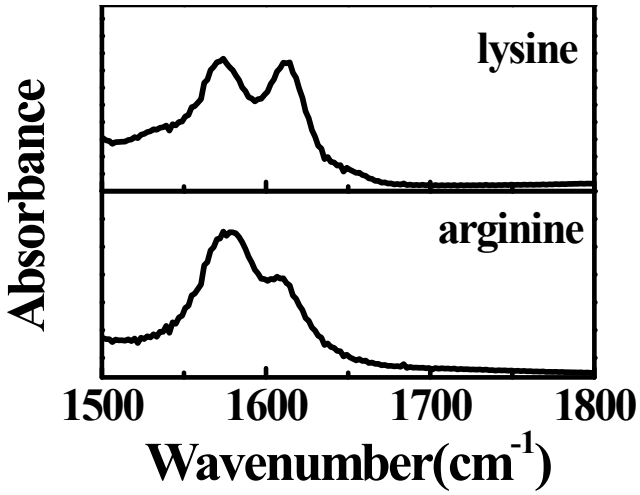

Figure S6. ATR-FTIR spectra of lysine (top) and arginine (bottom) in D_2O solutions at 1500-1800 cm^{-1}.

8. Experimental explanation for the non-resonant background drop after the introduction of lysine into the subphase of the lipid bilayer

The non-resonant background drop after the introduction of lysine into the subphase of d-DPMC bilayer in Figure 7A is actually associated with the interfacial water molecules. To help demonstrate our statement, we made a simple experiment by replacing the membrane-attached prism with a clean prism to monitor the single-point ssp SFG signal of 3200 cm^{-1} as a function of time as shown in Figure S7. Upon the addition of lysine, the intensity at 3200 cm^{-1} immediately dropped to a constant close to zero, whereby the signal at 3200 cm^{-1} is solely contributed by water molecules.[9,10] Given the fast diffusion process of positively charged lysine molecules into the

interfacial region between weakly positively charged CaF_2 prism and bulk water, it is reasonable to speculate that lysine can also reach the lipid bilayer interface and occupy the positions of membrane-bound water. Actually, such non-resonant background drop after addition of the amino acids is also observed in the d-DMPG bilayer(Figure S4). Therefore, the drop in the non-resonant background in Figure 7A is because the background of the water signal drops.

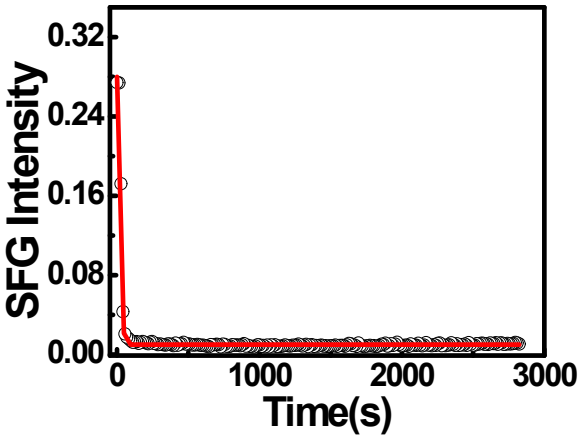

Figure S7. Time-dependent ssp SFG intensity at 3200 cm^{-1} at membrane-free prism/DI water interface upon the addition of lysine at t = 0 min.

9. The ssp SFG signals of d-DMPC/d-DMPC bilayer in the CD region before and after the injection of MP or 6-KC[11,12]

In Figure S8, the resonant SFG signals from the bilayer can be clearly observed after the strong interactions between d-DMPC/d-DMPC bilayer and the peptide/cholesterol.

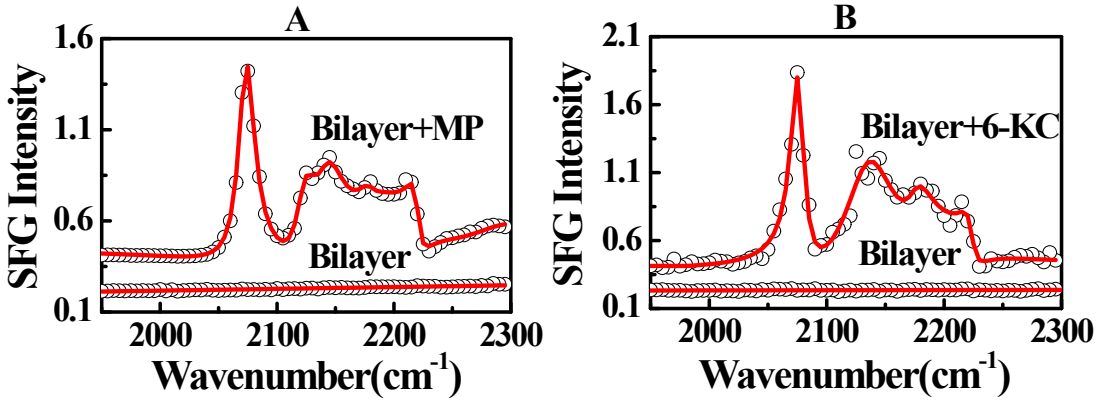

Figure S8. The ssp SFG spectra of d-DMPC/d-DMPC bilayer in the CD region before

and after the injection of MP (Figure S8A) or 6-KC (Figure S8B). (Figure S8A reproduced with permission from 2015, 119, 28523-28529, Copyright 2015, J. Phys. Chem. C., and Figure S8B reproduced with permission from 2014, 5, 419-424, Copyright 2014, J. Phys. Chem. Lett.)

10. The possible phase signs for the non-resonance, CD_3 group, CD_2 group and water background

As we were executing fitting operations on Figures 2 and 3, we found interesting variations in the phase signs in parallel with the evolution of the time-dependent SFG spectra. The phase signs were determined after considering all possible combinations of the phase signs. Only one combination fits our results, which is also proven by simulated SFG spectra in the CD region that show all possible combinations of the phase signs(Table S1) for the non-resonance, CD_3 group, CD_2 group and water background. The simulated spectra are given by Figure S9. It can be seen that only the cases of Figure S9a and S9e match well with the spectra before and after the addition of amino acid.

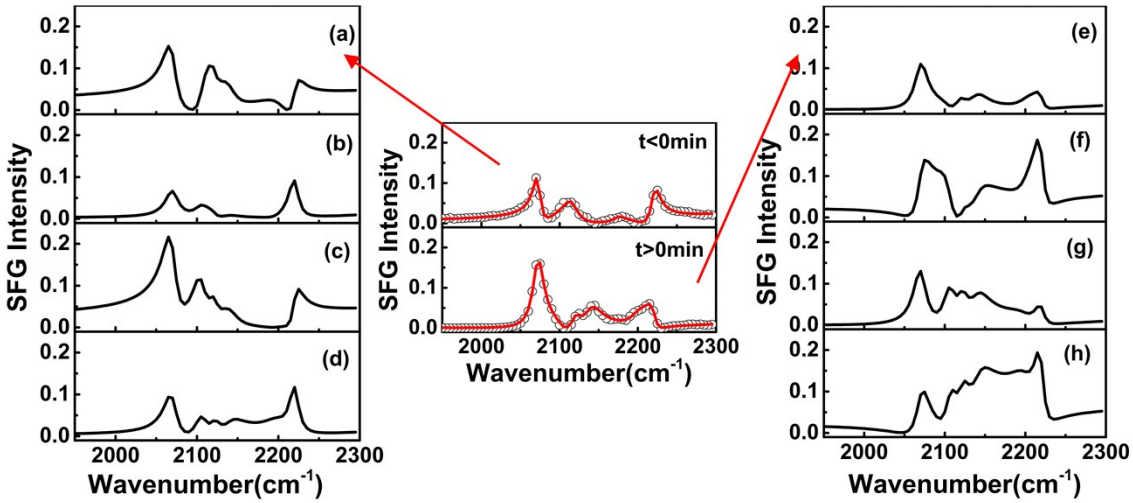

Figure S9. Left and right: Simulated SFG spectra with different phase sign combinations as listed in Table S1. Middle: Experimental SFG spectra before (top) and after (bottom) the introduction of amino acid into the subphase of d-DMPG lipid bilayer.

Table S1. Fitting parameters for simulated SFG spectra in Figure S9.

ω_ν	A_ν	Γ_ν	Phase sign							
			(a)	(b)	(c)	(d)	(e)	(f)	(g)	(h)
$\chi_{NR}^{(2)}$	0.1	/	-	-	-	-	+	+	+	+
2070	3	10	+	+	+	+	+	+	+	+
2105	2	10	-	-	+	+	-	-	+	+
2121	0.7	7	+	+	+	+	+	+	+	+
2140	2	15	+	+	+	+	+	+	+	+
2200	1	15	+	+	-	-	+	+	-	-
2220	1.8	7	-	-	-	-	-	-	-	-
2500	40	200	+	-	+	-	+	-	+	-

REFERENCES

1 X. Chen, J. Wang, C. B. Kristalyn, Z. Chen, *Biophys. J.,* 2007, **93**, 866-875.

2 Y. R. Shen, *The Principles of Nonlinear Optics*; Wiley: New York, **1984**.

3 A. G. Lambert, P. B. Davies, D. J. Neivandt, *Appl. Spectrosc. Rev.,* 2005, **40**, 103-145.

4 E. T. Castellana, P. S. Cremer, *Sur. Sci. Rep.,* 2006, **61**, 429-444.

5 S. J. Ye, K. T. Nguyen, S. V. Le Clair, Z. Chen, *J. Struct. Biol.,* 2009, **168**, 61-77.

6 H. F.Wang, W. Gan, R. Lu, Y. Rao, B. H. Wu, *Int. Rev. Phys. Chem.,* 2005, **24**, 191-256.

7 S.Gopalakrishnan, D. Liu, H. C.Allen, M. Kuo, M. J. Shultz, *Chem. Rev.,* 2006, **106**, 1155-1175.

8 G. Ma, H. C. Allen, *Langmuir,* 2006, **22**, 5341-5349.

9 V. Ostroverkhov, G. A. Waychunas, Y. Shen, *Chem. Phys. Lett.,* 2004, **386**, 144-148.

10 I. Li, J. Bandara, M. J. Shultz, *Langmuir,* 2004, **20**, 10474-10480.

11 J. Tan, S. J. Ye, Y. Luo, *J. Phys. Chem. C,* 2015, **119**, 28523-28529.

12 S. Ma, H. Li, K. Tian, S. Ye, Y. Luo, *J. Phys. Chem. Lett.,* 2014, **5**, 419-424.